Expression of Myelin Basic Protein Isoforms in Nonglial Cells

Susan M. Staugaitis,* P. R. Smith,* and David R. Colman

*Department of Cell Biology, New York University School of Medicine, New York 10016; and Departments of Anatomy and Cell Biology, and Pathology, Columbia University, College of Physicians and Surgeons, New York 10032

Abstract. The myelin basic proteins (MBPs) mediate the cytoplasmic apposition of the oligodendrocyte plasma membrane to form the major dense line of central nervous system myelin. Four major isoforms of murine MBP, obtained by alternative splicing of seven exons from a single primary transcript, display distinct developmental profiles. We expressed these major MBPs individually in HeLa cells and mapped their distributions by immunofluorescence and confocal microscopy. The 14- and 18.5-kD MBPs that are the predominant forms in compact myelin distributed primarily in the perinuclear regions of the cell in configurations highly suggestive of close association with membranes. We infer that these MBP isoforms possess strong, nonspecific membrane-binding properties that have been adapted by the oligodendrocyte to mediate compaction of the sheaths of plasma membrane that form myelin. In contrast, the 17- and 21.5-kD isoforms distributed diffusely in both the cytoplasm and the nucleoplasm and often accumulated within the nucleus. This distribution can be correlated with the presence of the peptide segment encoded by exon II, which is unique to these isoforms. The physiological significance of the nuclear targeting displayed by the 17- and 21.5-kD MBP isoforms in HeLa cells remains to be determined.

THE major dense line of myelin forms as the cytoplasmic surfaces of the expanding myelinating process are brought into close apposition (for review, see reference 35). The myelin basic proteins (MBPs)[1] are a set of peripheral membrane proteins that are known to play an essential role in the formation and maintenance of this structure (12, 34, 36). However, due to the rapidity with which myelin membranes wrap and compact (4, 9), the mechanisms by which the MBPs associate with the cytoplasmic surface of the forming myelin membrane cannot be easily studied. One model for this process postulates the existence of a myelin-specific receptor molecule for MBP (3, 20). A possible candidate is the proteolipid protein, that is present in myelin in an equimolar ratio with MBP (40) and possesses at least one domain exposed on the intracellular side of the bilayer (22). However, in dysmyelinating rats and mice in which proteolipid protein cannot be detected by immunocytochemistry, MBP can be localized within the sparse central nervous system myelin that does form, and ultrastructurally, a normal major dense line is observed (14, 15).

An alternative model proposes that MBP interacts directly with the lipid components in the myelin membrane (6, 42). It is well known that these highly charged peripheral membrane proteins are capable of avidly binding to a variety of natural and artificial membranes in vitro (42, for review see 6). MBP has a high affinity for acidic phospholipids (5, 11, 33), which are common constituents of all cellular membranes (23). Based on these properties, it might be expected that the MBPs would be found associated with various nonmyelin intracellular membranes and vesicles in the oligodendrocyte; however, this is not the case. There is strong evidence that free polysomes synthesizing MBP are selectively sequestered within actively myelinating zones of the oligodendrocyte processes (9, 24, 45, 46). The spatial segregation of MBP synthesis only to those regions where myelin is forming is believed to provide a specific targeting mechanism for MBP to myelin (9, 45). At the same time, the association of the newly synthesized polypeptides with other cellular membranes is prevented (9).

In mice and rats, four major MBP isoforms have been identified that can be separated by SDS-PAGE; their molecular weights are 21.5, 18.5, 17, and 14 kD (1, for review, see 7). These isoforms are obtained by translation of independent mRNAs (9, 49) that are alternatively spliced from a single primary transcript containing the seven exons of the MBP gene (10, 44). Exons I, III, IV, V, and VII are common to all four major isoforms; exon II is found in the 17- and 21.5-kD isoforms, and exon VI is unique to the 18.5- and 21.5-kD MBPs. A second 17-kD isoform containing exon VI, but lacking exons II and V, has also been described (32). The best evidence indicates that this isoform is five times less abundant than the 17-kD isoform containing exon II (32). The biological significance of the different MBP isoforms is unknown, but during myelinogenesis, there is a dramatic increase in the synthesis of the 14- and 18.5-kD forms (2). Because of their great abundance in adult myelin, all of the information about the biochemistry of the MBPs is from work with these two most abundant forms. The isolation of com-

1. *Abbreviation used in this paper*: MBP, myelin basic protein.

plete cDNA clones for each MBP isoform allows us to express even the less abundant forms at high levels, and so their individual properties are now accessible for study.

We have expressed four MBP isoforms individually by cDNA transfection in HeLa cells and mapped their distributions by immunofluorescence and confocal microscopy (47). The distributions fall into two distinct patterns that can be correlated with the presence or absence of the peptide sequence encoded by exon II of the MBP gene. Our data suggest that these two sets of isoforms have different membrane-binding properties that are likely to be physiologically significant in the developing oligodendrocyte.

Materials and Methods

Plasmid Constructions

The cDNA encoding the 14-kD rat MBP has been previously described (29). The cDNAs pM23-900, pM72, and pM44, encoding the 14-, 17-, and 21.5-kD mouse MBPs, respectively, were gifts from A. T. Campagnoni (University of California at Los Angeles, Los Angeles, CA), and the cDNA pHF43, encoding the 18.5-kD mouse MBP, was a gift from R. A. Lazzarini (Mount Sinai School of Medicine, New York, NY). For in vitro transcriptions, all of these cDNAs were subcloned into vectors of the pGEM series (Promega Biotec, Madison, WI) except pM23-900 which was acquired in a suitable transcription vector (Bluescribe M13+; Stratagene Cloning Systems, La Jolla, CA). For transfection experiments, cDNAs were subcloned into the pECE vector (16) which has the SV40 early promoter and polyadenylation signal flanking a multiple cloning region. All inserts, except for the 14-kD rat MBP cDNA, were subcloned directly into unique Eco RI sites in these vectors. The cDNA for the 14-kD rat MBP was incomplete at the 5′ end, and so an oligonucleotide adapter was added that extended from the Bam HI site in exon I of the cDNA to an artificial Hind III site located 11 base pairs upstream of the translation start codon. The naturally occurring 5′ nontranslated sequence immediately upstream from the start codon (38) was replaced by the sequence "CCACC". In this position this sequence acts to increase efficiency of translation initiation (for review, see 27). To permit subcloning of this cDNA into the vectors described above, the 3′ nontranslated region was truncated by digestion with Hinc II, which generated a blunt end. Hind III linkers were ligated onto the cDNA and digested to generate an insert of 643 bp. This was ligated to the unique Hind III sites in pGEM3 and pECE and oriented by restriction enzyme digestion. A schematic diagram of these cDNAs, including the exon representation of the four MBPs studied, is presented in Fig. 1 (*top*).

All of the plasmids were used to transform HB101 cells. Large scale preparations of these plasmids were obtained by alkaline lysis, RNase digestion, and purification on two sequential cesium chloride gradients (28).

In Vitro Transcription and Translation

In vitro transcriptions were performed on linearized plasmids using the appropriate bacteriophage RNA polymerase (either the SP6 or T7) and reaction kit obtained from Promega Biotec. Transcriptions were performed (37°C, 1 h) according to the manufacturer's recommendations with the addition of 0.5 mM $m^7G(5')ppp(5')G$ (Pharmacia Fine Chemicals, Piscataway, NJ) and 1 μCi ^3H ATP (specific activity >25 Ci/mmol) per reaction. The efficiency of the reactions were monitored by precipitation of mRNA with TCA followed by scintillation counting (28). The size of the transcripts was determined by electrophoresis in formaldehyde agarose gels (28) and fluorography using EN^{3}HANCE (Du Pont/New England Nuclear Research, Boston, MA).

mRNAs transcribed in vitro were used to program in vitro reticulocyte lysates containing 50 μCi [^{35}S]methionine (specific activity >1,000 Ci/mmol, Du Pont/New England Nuclear Research). Immunoprecipitates were prepared using polyclonal antiserum to MBP (9). Immune complexes were retrieved with protein A Sepharose (Sigma Chemical Co., St. Louis, MO) and separated on 15% SDS polyacrylamide gels followed by fluorography.

Transfections

HeLa cells, a cell line derived from a human cervical carcinoma, were cultured in DME supplemented with 7.5% FCS, 100 U/ml penicillin, 100 μg/ml streptomycin, and 2 mM glutamine (Gibco Laboratories, Grand Island, NY). 2 d before transfection, cells were trypsinized and 1.5×10^4 cells were plated onto coverslips placed in 24-well dishes and precoated with 10 μg/ml poly-l-lysine (P2636; Sigma Chemical Co.). This procedure yielded coverslips that were 70–80% confluent on the day of transfection. In early experiments, calcium phosphate precipitates were prepared (48) using 25–50 μg of DNA and diluted in medium so that 1–2 μg of DNA was applied to each coverslip. Cells were incubated at 37°C for 5 h, incubated with 15% glycerol in complete medium for 30 s, washed twice, and incubated overnight in complete DME containing 5 mM sodium butyrate (Sigma Chemical Co.) to enhance expression of the transfected DNA (21). In later experiments, liposome-mediated transfections (lipofections) were performed (17). Lipofectin reagent (BRL Life Technologies, Gaithersburg, MD) was diluted in Opti-MEM (Gibco Laboratories) to a final concentration of 5 μg/ml and mixed with an equal volume of DNA diluted to 4 μg/ml in Opti-MEM and incubated for 10 min at room temperature. 1 ml of this mixture was added to each coverslip, which had been washed twice with Opti-MEM. The cells were incubated for 5 h at 37°C and then given complete DME containing 5 mM sodium butyrate. 24 h after addition of DNA the cells were processed for immunofluorescence staining.

Affinity Purification of Antiserum to MBP

Rat MBP was prepared by partial delipidation of myelin, extraction at pH 2, and precipitation in 11 vol of acetone at −20°C. After sedimentation, the pellet was resuspended in 0.05 M sodium phosphate buffer, pH 6.3, coupled to 0.5 ml of Affigel 10 (Bio-Rad Laboratories, Richmond, CA), and used for affinity purification of a rabbit polyclonal antiserum to MBP (9).

Immunofluorescence

The cells were washed with Dulbecco's PBS, fixed with 4% paraformaldehyde in PBS, washed with PBS, permeabilized using 0.1% Triton X-100, and blocked with PBS containing 0.2% gelatin. Cells were incubated with affinity-purified antiserum diluted 1:50 in PBS-gelatin solution for 1 h, followed by washing with PBS-gelatin, and incubation with either TRITC-conjugated (Organon Teknika Corp., West Chester, PA) or FITC-conjugated (Kirkegaard & Perry Laboratories, Inc., Gaithersburg, MD) second antibody using the same conditions. After washing, coverslips were mounted onto slides for epifluorescence using a microscope (Dialux 20; E. Leitz, Inc., Rockleigh, NJ). When FITC-labeled coverslips were prepared for confocal microscopy, *n*-propyl gallate (2%) (19) was included in the mounting medium to retard photobleaching.

Confocal Microscopy

Confocal imaging of FITC-stained coverslips was performed using PHOIBOS 1000 confocal microscopy (Sarastro Inc., Sweden) based on a microscope using a 63×/1.4 Planapochromat lens (Universal Model, Carl Zeiss, Inc., Thornwood, NY). 512 × 512 images were recorded of a 180-μm^2 field. Serial optical sections were taken at 1-μm increments. Usually two to three scans of the same level in the specimen were averaged to help reduce noise. The number of images averaged was selected to minimize bleaching of the entire sample during the recording process. Three-dimensional images were stored on a hard disk of a MicroVAX II computer (Digital Equipment Corp., Maynard, MA) and displayed using an image processor (model IP8500; Gould Imaging and Graphics Division, Fremont, CA or model Lex 90; Adage Inc., Billerica, MA) attached to the MicroVAX. Image processing was performed using the Micrograph Data Processing Program (41) and consisted of contrast enhancement and pseudocolor display adjustments to optimally visualize subcellular features. Black and white images were photographed directly from the Lex 90 monitor using a 135-mm Nikkormat telephoto lens and TMax 100 film (Eastman Kodak Co., Rochester, NY). Color photographs were taken using a Freeze-Frame Image Recorder (Polaroid, Cambridge, MA) and film (Ektachrome EN 135 100; Eastman Kodak Co.)

In Vitro Translation of Brain mRNA

Brains from 0- or 60-d-old rats were homogenized in guanidinium hydrochloride and total RNA was extracted as described (9). Wheat germ translation mixtures with [^{35}S]methionine (100 μCi) included were programmed with 10 μg total RNA per 25 μl translation for 3 h at 25°C (9). Immunoprecipitates using a polyclonal antiserum to MBP and translation volumes containing 2.4×10^6 TCA-precipitable cpm were prepared and subjected to SDS-PAGE and fluorography (9).

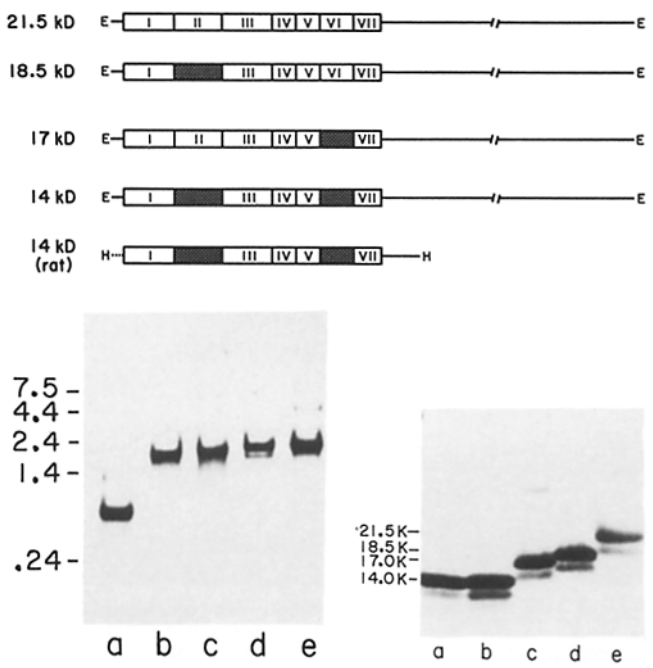

Figure 1. Characterization of cDNA clones used in transfection experiments. (*top*) Schematic diagram of MBP cDNA inserts showing the exon representation for each isoform. Thick bars represent the translated region of the cDNAs, and lines represent the nontranslated regions. The 5′ nontranslated region is encoded by exon I, and the 3′ nontranslated region is encoded by exon VII. The shaded rectangles denote absent exons in the cDNAs. All cDNAs are from mouse except where indicated. The 3′ nontranslated region is ~1,500 bp long in the mouse cDNAs, whereas the 3′ nontranslated region in the rat cDNA is ~250 bp long. The 5′ nontranslated region of this cDNA was modified (see Materials and Methods). *E*, Eco RI; H, Hind III. (*bottom left*) In vitro transcription of MBP cDNAs. Plasmids were linearized at the 3′ end of the insert, transcribed in the presence of appropriate DNA polymerase and [^{3}H]-ATP, separated by electrophoresis in formaldehyde agarose gels, and radioactivity was detected by fluorography. (*a*) 14 kD MBP from rat; (*b*) 14 kD MBP; (*c*) 17 kD MBP; (*d*) 18.5 kD MBP; and (*e*) 21.5 kD MBP. The mRNAs synthesized are the correct predicted sizes. (*bottom right*) In vitro translation. mRNA from in vitro transcriptions in *b* were used to program reticulocyte lysates containing [^{35}S] methionine. Immunoprecipitates were prepared using polyclonal antiserum to MBP. (*a*) 14 kD MBP from rat; (*b*) 14 kD MBP; (*c*) 17 kD MBP; (*d*) 18.5 kD MBP; and (*e*) 21.5 kD MBP. All proteins synthesized are the correct predicted sizes. The minor, fast migrating MBP bands probably represent initiation at an in-frame internal AUG. This band is much reduced in the 14-kD rat MBP in which the 5′ nontranslated region was modified to enhance translational efficiency (see Materials and Methods).

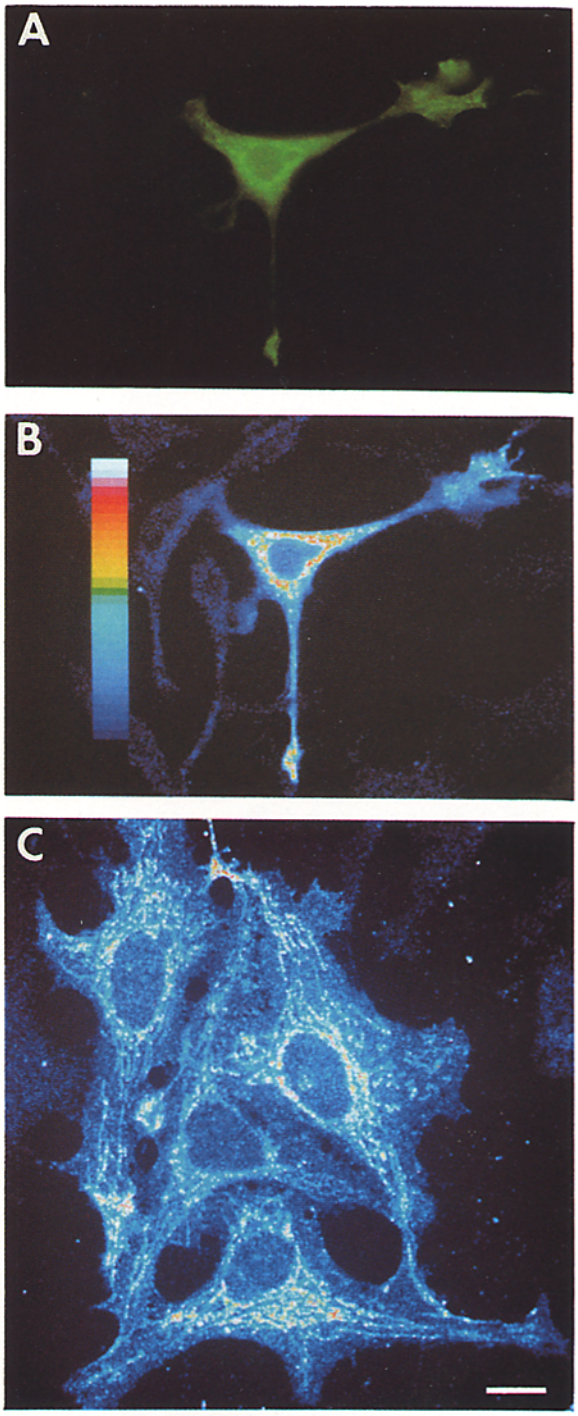

Figure 2. Conventional and confocal fluorescence imaging of the 14-kD rat MBP expressed by transfection of HeLa cells. Expression was detected by indirect immunofluorescence as described in Materials and Methods. Conventional epifluorescence (*A*) and confocal (*B*) images were recorded from the same cell. Optical sectioning by confocal microscopy (*B*) demonstrates that the perinuclear fluorescence intensity observed in *A* represents a restricted distribution of the 14-kD MBP. (*C*) This image shows the reticular distribution observed in cells that express the 14-kD MBP. White represents the highest intensity of fluorescence on the color scale. Bar, 20 μm.

Results

In Vitro Transcription and Translation of cDNA Clones

The exon organization of the cDNA inserts encoding the major isoforms of MBP are diagrammed in Fig. 1 (*top*). In vitro transcription of each cDNA, followed by formaldehyde gel electrophoresis, showed that the transcribed mRNAs obtained are the correct predicted sizes (Fig. 1, *bottom left*). The small size differences between the individual full-length MBP mRNAs are evident and represent the presence or ab-

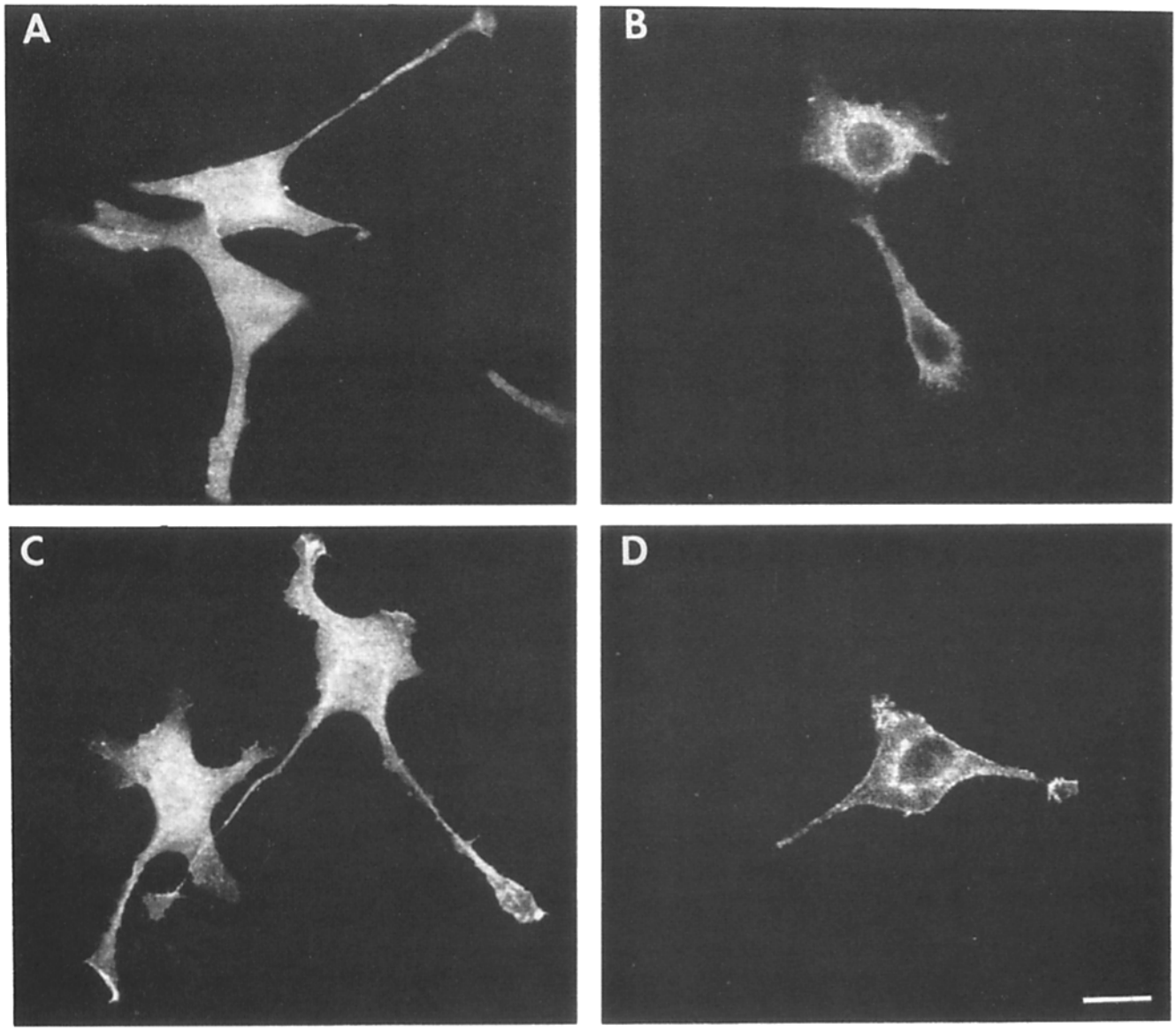

Figure 3. Distribution of the individual mouse MBP isoforms when expressed in HeLa cells. Cells are stained as described in Materials and Methods and imaged using confocal microscopy. (*A*) 21.5 kD MBP; (*B*) 18.5 kD MBP; (*C*) 17 kD MBP; and (*D*) 14 kD MBP. The 14- and 18.5-kD isoforms are concentrated in the perinuclear region of the cytoplasm, whereas the 17- and 21.5-kD MBPs are uniformly distributed throughout the cytoplasm and nucleoplasm. Bar, 20 μm.

sence of exons II and VI in the transcripts. All proteins obtained by in vitro translation of these transcripts had the identical electrophoretic mobility as the homologous proteins in rat myelin (data not shown) and were immunoprecipitable with antiserum to MBP (Fig. 1, *bottom right*). As expected, the rat MBP cDNA, which was truncated in the 3′ nontranslated region, encoded a protein the same size as the cDNA for the mouse 14-kD MBP which was full length. All MBP translation products contained minor bands that migrated slightly faster than the major band. This probably represents initiation at an in frame internal AUG (methionine, amino acid 19) that lies within exon I and so is common to all MBP isoforms. This product was greatly reduced in the 14-kD rat MBP, the cDNA in which the 5′ end had been modified to give a highly preferred translation initiation site (see Materials and Methods).

Expression of MBP cDNAs in HeLa Cells

Expression in HeLa cells of the transfected cDNAs was first detectable by immunofluorescence at 9 h after application of cDNA, and the highest number of positive cells were observed at 24 h. No positive cells were observed when cDNA was omitted from the experiment. The distributions described below were typically seen at all time points. Transfection efficiencies for each cDNA ranged from 1 to 10% and appeared to depend upon the purity of the DNA preparation. In general, there was no difference in transfection efficiency or in overall levels of expression between cells transfected using calcium phosphate precipitates or lipofection techniques. Lipofection was preferable because higher transfection efficiencies were consistently reproducible and, since it was technically easier to perform scaled-down transfections using lipofection, DNA was conserved. We treated the cells

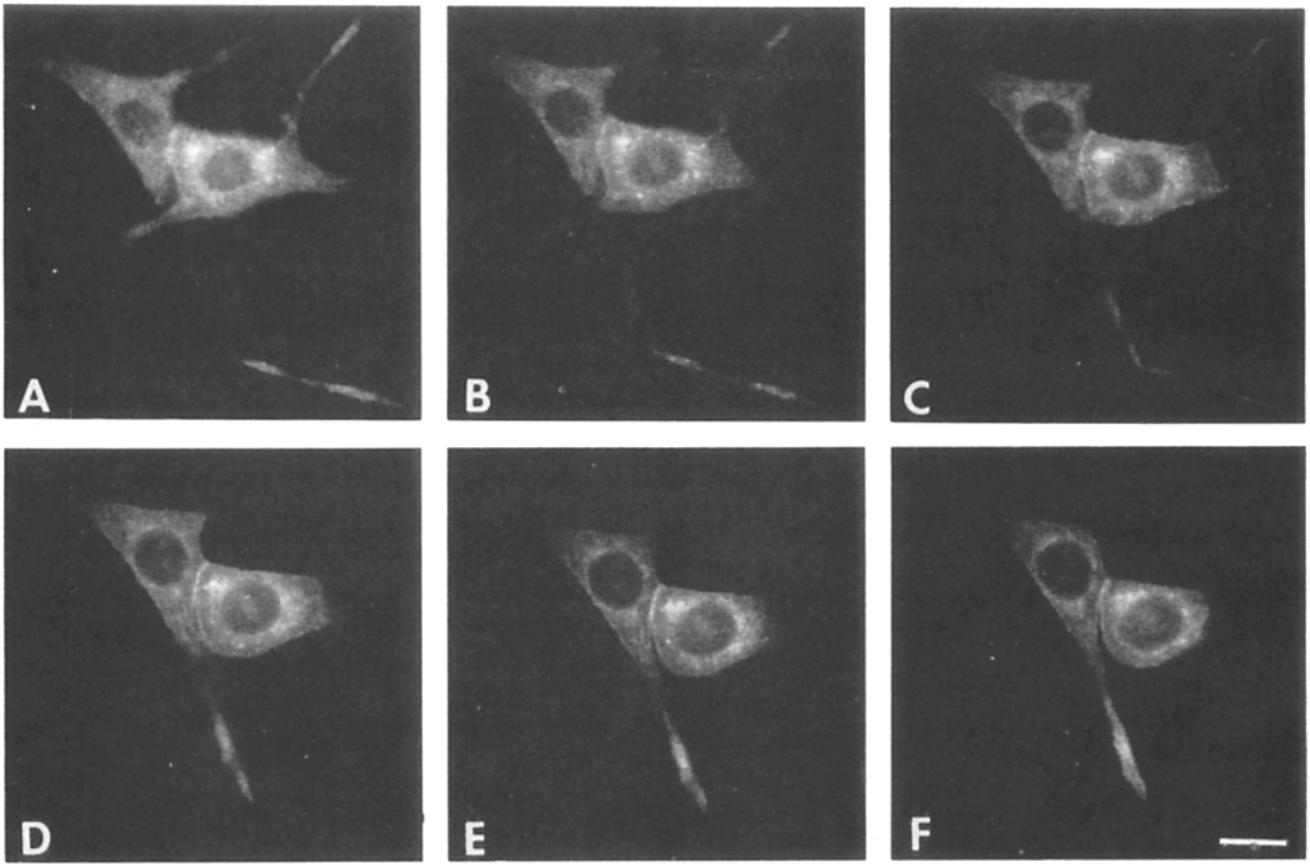

Figure 4. Optical sectioning of two HeLa cells expressing the 14-kD mouse MBP. Images were recorded starting at a level near the coverslip on which the cell was grown (*A*) and repeated at five additional consecutive 1-μm increments towards the top of the cells (*B–F*). Intense immunofluorescence in the perinuclear region is observed at all levels of the cells. Bar, 20 μm.

with sodium butyrate, which has been shown to increase both the number of expressing cells and the absolute level of expression within individual cells (21). This treatment also caused the HeLa cells to become more stellate, with extended processes.

Subcellular Distribution of MBP Isoforms in Transfected HeLa Cells

The 14-kD rat MBP, when expressed in HeLa cells, displayed a highly restricted distribution (Fig. 2 *A*). The highest intensity of fluorescence was always in the perinuclear region of the cell whether the cells were expressing at high or low levels. In many cells, the fluorescence was clumped or granular in appearance. Although the perinuclear intensity in cells expressing the 14-kD MBP was obvious and reproducible, it was possible that this fluorescence did not represent a restricted distribution of MBP, but merely reflected the greater cell thickness in this region. To more precisely map the distribution of transfected MBPs, we viewed these cells using a confocal microscope. Confocal imaging eliminates light above and below the plane in focus, so it is possible to view individual optical sections within the cell (see 47). The thickness of each optical section in the system we used was less than 1 μm. Since HeLa cells are 8–12 μm thick, several sections through the cell were obtained, and the distribution of the expressed proteins were accurately mapped at each level within the cell. Fig. 2 *B* shows a confocal optical section of the cell viewed by conventional fluorescence microscopy in Fig. 2 *A*. The optical section was taken through the nucleus at a level close to the coverslip on which the cells were grown. The image is presented using a color scale in which black represents the least intense, and white, the most intense fluorescence. This optical section clearly shows that the 14-kD rat MBP is localized predominantly in the perinuclear region with much less fluorescence in other areas (Fig. 2 *B*). The clumped, granular appearance of the fluorescent label was much more obvious in optical sections than it was by conventional fluorescence microscopy. In cells expressing MBP apparently at lower levels, a lacelike reticular pattern extending into the peripheral regions of the cells could be discerned (Fig. 2 *C*).

A perinuclear distribution was also observed when the full length cDNAs encoding the 14- and 18.5-kD MBPs from mice were expressed individually in HeLa cells (Fig. 3, *B* and *D*). In addition, confocal imaging often revealed increased fluorescence at the plasma membrane which was observed most frequently in cells expressing the mouse 14-kD MBP (Figs. 3 *D* and 4). The same patterns were obtained through serial optical sections of the cells (Fig. 4).

The distribution of the 17- and 21.5-kD MBP isoforms were markedly different from the 14- and 18.5-kD isoforms but identical to each other (Fig. 3, *A* and *C*). Commonly, the dis-

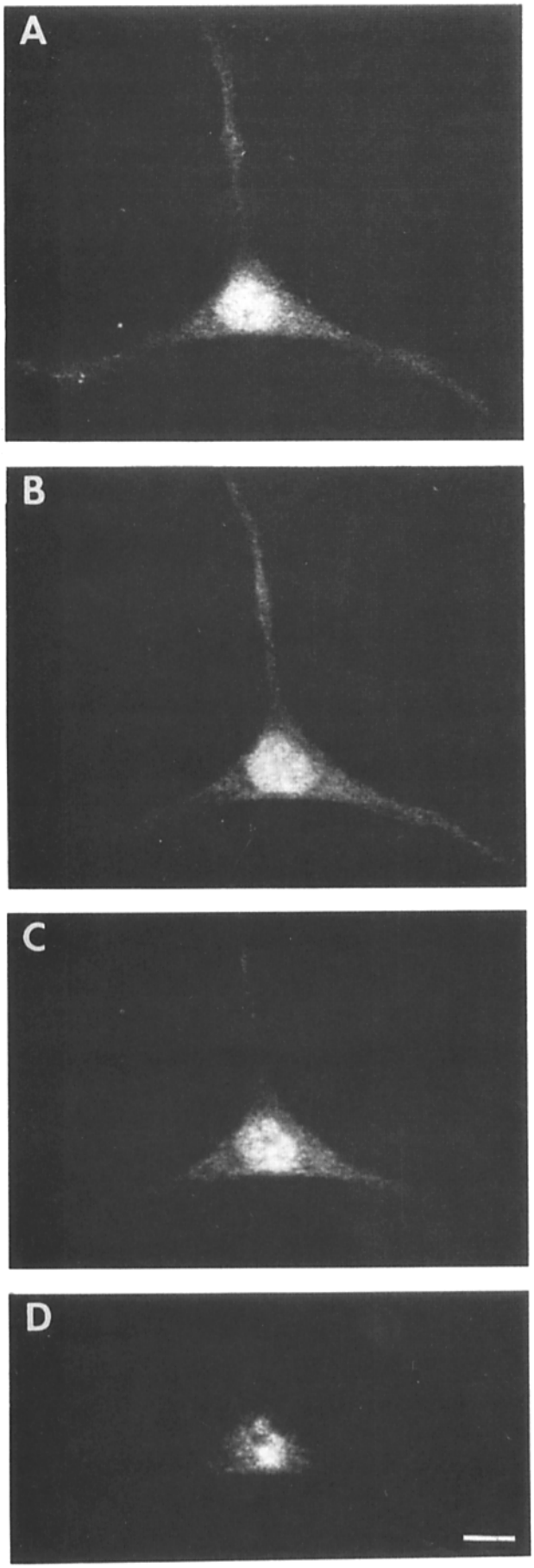

tribution was uniform throughout the cell including the nucleus. Frequently, no nuclear outline could be detected in confocal sections, although in phase contrast, normal appearing nuclei were plainly visible (data not shown). In other cells, label inside the nucleus exceeded that observed in the cytoplasm (Fig. 5). Sometimes, the nucleoli were the most intensely fluorescent parts of the cell, but in other cells, nucleoli were not labeled. Nuclear fluorescence was not seen to any significant extent in cells expressing the 14- and 18.5-kD isoforms of MBP, even when these cells were expressing these proteins at very high levels. In a few cells expressing at low levels, the 17- and 21.5-kD isoforms were found homogeneously within the cytoplasm but not within the nucleus.

In Vitro Translation of Brain mRNA

The developmental change in MBP isoform expression is shown in Fig. 6. The difference in intensity of the bands between lane *a* and *b* reflects the overall increased abundance of translatable MBP mRNA in the adult animal compared with the neonate. Densitometric scans of the autoradiogram reveal that the 17- and 21.5-kD MBP isoforms represent ~25% of the MBP complement in newborn rats (Fig. 6, lane *a*), whereas in the adult (Fig. 6, lane *b*) these isoforms are very low in abundance and the 14- and 18.5-kD isoforms are the predominant isoforms.

Discussion

Progress towards understanding the subcellular mechanisms by which the MBPs are synthesized and interact with the membrane of the myelinating process to mediate the formation of the major dense line has been slow because this is a very rapid event, and therefore is difficult to study. Kinetic experiments reveal that MBPs enter myelin virtually instantaneously after synthesis (4, 9). This is almost certainly due to the placement of MBP synthesizing polysomes selectively within myelinating zones (9, 24, 45, 46), as well as to the reactive properties of the polypeptides themselves (5, 6, 11, 33, 42). In the transfected cell system presented here, each MBP isoform displays properties that may be interpreted in light of what is known about the distribution of the MBPs in oligodendrocytes in vivo.

The 14- and 18.5-kD MBP Isoforms Appear to Bind to Intracellular Membranes

In most HeLa cells, the 14- and 18.5-kD MBPs were distributed at the highest levels in the perinuclear regions (Figs. 2, 3, *B* and *D*, 4). This fluorescence pattern is highly reminiscent of the distributions of both resident ER proteins, such as endoplasmin (26) and Ig heavy chain binding protein (31), as well as that of other proteins known to be synthesized on

Figure 5. Optical sectioning of HeLa cell expressing the 21.5-kD mouse MBP. Images were recorded starting at a level near the coverslip on which the cell was grown (*A*) and repeated at three additional consecutive 1-μm increments towards the top of the cell (*B–D*). Intense nuclear fluorescence is observed in all optical sections. Bar, 20 μm.

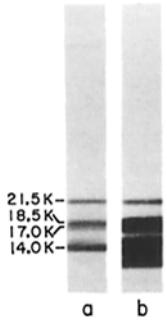

Figure 6. Developmental profile of the MBP isoforms. Total RNA from 0 d- (*a*) and 2-mo- (*b*) old rat brains was used to program wheat germ translation mixtures containing ^{35}S-labeled methionine. Immunoprecipitates using antiserum to MBP were prepared from translation volumes containing 2.4 × 10^6 TCA-precipitable cpm, separated by SDS-PAGE, and visualized by fluorography. This fluorogram was exposed to reveal the 21.5-kD MBP species. At shorter exposures, the strong 18.5-kD and the faint 17-kD bands in lane *b* can be resolved. The 13-kD band visible in lane *b* is an inconstant feature of MBP immunoprecipitates from in vitro translation mixtures. This band is likely to be the result of initiation at an in-frame internal AUG in the 14-kD MBP mRNA.

the ER, but targeted to other subcellular locations such as the plasma membrane (for example, see 18). This "ER-like" distribution found for the 14- and 18.5-kD MBPs is perhaps best shown in Fig. 2 *C*, where a lacelike reticulum delineated by MBP immunofluorescence is concentrated in the perinuclear region and extends well into the cell processes. Although in our experiments there are strong similarities in intracellular distribution between the 14- and 18.5-kD MBP isoforms and proteins synthesized in the RER, it has been demonstrated that the MBPs are synthesized on free polysomes (8, 9). Therefore, the distribution of MBP most likely reflects an association of the 14- and 18.5-kD isoforms with the cytoplasmic face of perinuclear membranes which can include the RER, Golgi apparatus, associated transport vesicles, and perhaps mitochondria. In fact, biochemical experiments have shown that the bovine 18.5-kD isoform avidly binds to phospholipid membrane vesicles and causes their aggregation (42). These phenomena may be directly analogous to how MBP associates with the cytoplasmic aspect of the myelin bilayer.

The preponderance of MBP within the perinuclear region could arise if MBP mRNAs, after transport out of the nucleus, are rapidly incorporated into perinuclear polysomes and translated in that same region. The newly synthesized protein would be in a position to bind to nearby membranes, such as those of the RER that are concentrated in this vicinity (for example, see 26, 31). After attachment, a proportion of the MBP polypeptides might become passengers in the normal intracellular traffic and distribute to other membranous organelles of the cell. Indeed, we have observed what appear to be vesicular elements in the periphery of the cell (Figs. 2, 3, *B* and *D*, 4) and at the plasma membrane (Fig. 3 *D*, 4), although not at high concentration. Alternatively, the appearance of MBP at other sites within the cell could arise by initiation of translation near these sites. The association of the 14-kD MBP with cellular membranes has also been observed after subcellular fractionation of transfected Cos-1 cells (3). In these experiments, 80% of the MBP was distributed among all the fractions that contained membrane-bound organelles. The data therefore suggest that these isoforms of MBP, which are the most abundant isoforms in compact myelin, display membrane associations in HeLa cells similar to that observed in in vitro binding studies. The difference in distribution between MBP in HeLa cells and that in myelinating oligodendrocytes reflects the apparent absence in HeLa cells of a MBP mRNA segregation mechanism. One might envision that evolutionary acquisition of this mechanism allowed the development of highly reactive MBP isoforms.

The 17- and 21.5-kD MBP Isoforms Are Diffusely Distributed in Transfected HeLa Cells

The 17- and 21.5-kD MBP isoforms were diffusely distributed in the cytoplasm (Fig. 3, *A* and *C*), and surprisingly, in most cells, these proteins were detected within the nucleoplasm at levels that were often much higher than that observed in the cytoplasm (Fig. 5). Molecules in the size range of the MBPs have the ability to enter the nucleus passively by diffusion across nuclear pores (for review, see 13). If this is the mechanism by which these two isoforms enter the nucleus, then it might be expected that the 14- and 18.5-kD isoforms might localize in the nucleus as well were it not for their higher membrane affinities. The 17- and 21.5-kD MBPs apparently do not have this same affinity for membranes and so are free to diffuse throughout the cytoplasm and into the nucleus. Both of these isoforms contain the peptide sequence encoded by exon II of the MBP gene, while the 14- and 18.5-kD isoforms do not. The presence of this exon might result in a conformation that alters the membrane binding properties of the 17- and 21.5-kD isoforms.

The intranuclear accumulation of MBP observed in some cells might be mediated by a nuclear localization sequence (13, 25, 30, 37). These are typically stretches of seven amino acids rich in positively charged amino acids and proline; however, no single consensus sequence has been identified (13, 25, 30, 37). Two regions within the MBP sequence that bear strong similarities to known nuclear targeting signals in yeast histone H2B (30), polyoma virus T antigen (37), and SV40 T antigen (25) (Fig. 7) were identified by the BESTFIT program (UWGCG Package). These regions, one of which lies within exon I at the I/II border and the other, within exon VII, are common features of all MBP isoforms. The presence of exon II in the 17- and 21.5-kD isoforms might establish a conformation that exposes and thus "activates" the potential nuclear targeting signals. It is unknown whether any MBP is targeted to the nucleus of oligodendrocytes in vivo. If so, the possibility that certain MBP isoforms may have a regulatory role in myelin formation should be considered. On the other hand, interactions between the different

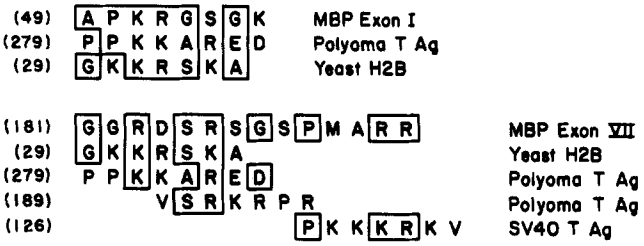

Figure 7. Potential nuclear targeting signals in the MBP sequence. Similarities between two peptide sequences in MBP and nuclear targeting sequences identified in yeast histone H2B (30), polyoma virus T antigen (37), and SV40 T antigen (25) are shown. Numbers in parentheses indicate the location of these sequences within their respective polypeptides.

MBP isoforms in oligodendrocytes may prevent the nuclear localization of exon II-containing isoforms.

Relevance to MBP Distribution in Developing Oligodendrocytes

The data presented here show that the subcellular distribution of the MBP isoforms in HeLa cells can be correlated with the presence or absence of the peptide sequence encoded by exon II. Early in myelinogenesis in vivo, the exon II containing 17- and 21.5-kD isoforms together represent ~25% of the total MBP complement (Fig. 6). At this time, oligodendrocytes are just forming processes, and there is little compact myelin (39, 43). Immunocytochemical staining of MBP before the deposition of myelin sheaths reveals homogeneous staining throughout the cell bodies and forming processes (39, 43). This is consistent with our experiments which demonstrated a diffuse distribution for these isoforms when expressed in transfected HeLa cells. Once compact myelin forms, however, all detectable MBP is in the myelin sheaths (39, 43). In 2-mo-old (adult) rodents, the isoforms that express exon II represent less than 5% of the total MBP complement (Fig. 6). Assembly of compact myelin is therefore accompanied by a dramatic increase in the synthesis of the 14- and 18.5-kD MBPs which in our experiments apparently have higher intracellular membrane-binding affinities. This is consistent with the finding that in all species studied to date, the major forms found in highly purified compact myelin are either the 14- or the 18.5-kD isoforms. These studies suggest that despite their extensive overall homology, the individual MBP isoforms display marked differences in properties that may be of functional significance in oligodendrocytes. Cotransfection of combinations of these isoforms into nonglial cells can be used to study whether coexpression of these isoforms can modify the properties observed when expressed individually.

We thank Anthony T. Campagnoni and Robert A. Lazzarini for providing us with the mouse MBP cDNAs; and Edie Abreu, Eric Hubel, and Katie Rosa for help in preparing the manuscript. We also thank David D. Sabatini, Gert Kreibich, and James L. Salzer for helpful discussions. This investigation was supported by National Institutes of Health (NIH) Grant NS20147 to D. R. Colman, National Multiple Sclerosis Society Grant RG2090 to D. R. Colman, NIH Training Grant 5T32GM07308 from the National Institute of General Medical Sciences to S. M. Staugaitis and National Science Foundation Grants DMB-8515392 and DIR-8908095 to P. R. Smith.

Received for publication 18 October 1989 and in revised form 16 January 1990.

References

1. Barbarese, E., P. E. Braun, and J. H. Carson. 1977. Identification of prelarge and presmall basic proteins in mouse myelin and their structural relationship to large and small basic proteins. *Proc. Natl. Acad. Sci. USA.* 74:3360-3364.
2. Barbarese, E., J. H. Carson, and P. E. Braun. 1978. Accumulation of the four myelin basic proteins in mouse brain during development. *J. Neurochem.* 31:779-782.
3. Barbarese, E., C. Barry, C.-H. J. Chou, D. J. Goldstein, G. A. Nakos, R. Hyde-DeRuyscher, K. Scheld, and J. H. Carson. 1988. Expression and localization of myelin basic protein in oligodendrocytes and transfected fibroblasts. *J. Neurochem.* 51:1737-1745.
4. Benjamins, J. A., R. Iwata, and J. Hazlett. 1978. Kinetics of entry of proteins into the myelin membrane. *J. Neurochem.* 31:1077-1085.
5. Boggs, J. M., M. A. Moscarello, and D. Papahadjopoulos. 1977. Phase separation of acidic and neutral phospholipids induced by human myelin basic protein. *Biochemistry.* 16:5420-5426.
6. Boggs, J. M., M. A. Moscarello, and D. Papahadjopoulos. 1982. Structural organization of myelin: role of lipid-protein interactions determined in model systems. *In* Lipid-Protein Interactions. P. C. Jost and O. H. Griffith, editors. John Wiley & Sons Inc., New York. 1-51.
7. Campagnoni, A. T. 1988. Molecular biology of myelin proteins from the central nervous system. *J. Neurochem.* 51:1-14.
8. Campagnoni, A. T., G. D. Carey, and Y.-T. Yu. 1980. *In vitro* synthesis of the myelin basic proteins: subcellular site of synthesis. *J. Neurochem.* 34:677-686.
9. Colman, D. R., G. Kreibich, A. B. Frey, and D. D. Sabatini. 1982. Synthesis and incorporation of myelin polypeptides into CNS myelin. *J. Cell Biol.* 95:598-608.
10. deFerra, F., H. Engh, L. Hudson, J. Kamholz, C. Puckett, S. Molineaux, and R. A. Lazzarini. 1985. Alternative splicing accounts for the four forms of myelin basic protein. *Cell.* 43:721-727.
11. Demel, R. A., Y. London, W. S. M. Geurts Van Kessel, F. G. A. Vossenberg, and L. L. M. van Deenen. 1973. The specific interaction of myelin basic protein with lipids at the air-water interface. *Biochim. Biophys. Acta.* 311:507-519.
12. Depouey, P., C. Jacque, J. M. Bourre, F. Cesselin, A. Privat, and N. Baumann. 1979. Immunochemical studies of myelin basic protein in *shiverer* mouse devoid of major dense line of myelin. *Neurosci. Lett.* 12:113-118.
13. Dingwall, C., and R. A. Laskey. 1986. Protein import into the cell nucleus. *Annu. Rev. Cell Biol.* 2:367-390.
14. Duncan, I. D., J. P. Hammang, and B. D. Trapp. 1987. Abnormal compact myelin in the myelin-deficient rat: absence of proteolipid protein correlates with a defect in the intraperiod line. *Proc. Natl. Acad. Sci. USA.* 84:6287-6291.
15. Duncan, I. D., J. P. Hammang, S. Goda, and R. H. Quarles. 1989. Myelination in the *jimpy* mouse in the absence of proteolipid protein. *Glia.* 2:148-154.
16. Ellis, L., E. Clauser, D. O. Morgan, M. Edery, R. A. Roth, and W. J. Rutter. 1986. Replacement of insulin receptor tyrosine residues 1162 and 1163 compromises insulin-stimulated kinase activity and uptake of 2-deoxyglucose. *Cell.* 45:721-732.
17. Felgner, P. L., T. R. Gadek, M. Holm, R. Roman, H. W. Chan, M. Wenz, J. P. Northrop, G. M. Ringold, and M. Danielsen. 1987. Lipofection: a highly efficient, lipid-mediated DNA-transfection procedure. *Proc. Natl. Acad. Sci. USA.* 84:7413-7417.
18. Gething, M.-J., and J. Sambrook. 1981. Cell-surface expression of influenza haemagglutinin from a cloned DNA copy of the RNA gene. *Nature (Lond.).* 293:620-625.
19. Giloh, H., and J. W. Sedat. 1982. Fluorescence microscopy: reduced photobleaching of rhodamine and fluorescein protein conjugates by *n*-propyl gallate. *Science (Wash. DC).* 217:1252-1255.
20. Golds, E. E. and P. E. Braun. 1978. Protein associations and basic protein conformation in the myelin membrane: the use of difluorodinitrobenzene as a cross-linking reagent. *J. Biol. Chem.* 253:8162-8170.
21. Gorman, C. M., B. H. Howard, and R. Reeves. 1983. Expression of recombinant plasmids in mammalian cells is enhanced by sodium butyrate. *Nucleic Acids Res.* 11:7631-7648.
22. Hudson, L. D., V. L. Friedrich, Jr., T. Behar, M. Dubois-Dalcq, and R. A. Lazzarini. 1989. The initial events in myelin synthesis: orientation of proteolipid protein in the plasma membrane of cultured oligodendrocytes. *J. Cell Biol.* 109:717-727.
23. Jain, M. K., and R. C. Wagner. 1980. Introduction to Biological Membranes. J. Wiley & Sons, Inc., New York. 25-52.
24. Jordan, C., V. Friedrich, and M. Dubois-Dalcq. 1989. *In situ* hybridization analysis of myelin gene transcripts in developing mouse spinal cord. *J. Neurosci.* 9:248-257.
25. Kalderon, D., B. L. Roberts, W. D. Richardson, and A. E. Smith. 1984. A short amino acid sequence able to specify nuclear location. *Cell.* 39: 499-509.
26. Koch, G. L. E., C. Booth, and F. B. P. Wooding. 1988. Dissociation and re-assembly of the endoplasmic reticulum in live cells. *J. Cell Sci.* 91: 511-522.
27. Kozak, M. 1989. The scanning model for translation: an update. *J. Cell Biol.* 108:229-241.
28. Maniatis, T., E. F. Fritsch, and J. Sambrook. 1982. Molecular Cloning: A Laboratory Manual. Cold Spring Harbor Laboratory, Cold Spring, NY. 545 pp.
29. Mentaberry, A., M. Adesnik, M. Atchison, E. M. Norgard, F. Alvarez, D. D. Sabatini, and D. R. Colman. 1986. Small basic proteins of myelin from central and peripheral nervous systems are encoded by the same gene. *Proc. Natl. Acad. Sci. USA.* 83:1111-1114.
30. Moreland, R. B., G. L. Langevin, R. H. Singer, R. L. Garcea, and L. M. Hereford. 1987. Amino acid sequences that determine the nuclear localization of yeast histone 2B. *Mol. Cell. Biol.* 7:4048-4057.
31. Munro, S., and H. R. B. Pelham. 1986. An Hsp70-like protein in the ER: identity with the 78 kd glucose-regulated protein and immunoglobulin heavy chain binding protein. *Cell.* 46:291-300.
32. Newman, S. L., K. Kitamura, and A. T. Campagnoni. 1987. Identification of a cDNA coding for a fifth form of myelin basic protein in mouse. *Proc. Natl. Acad. Sci. USA.* 84:886-890.
33. Palmer, F. B., and R. M. C. Dawson. 1969. Complex-formation between triphosphoinositide and experimental allergic encephalitogenic protein.

Biochem. J. 111:637–646.
34. Privat, A., C. Jacque, J. M. Bourre, P. Dupouey, and N. Baumann. 1979. Absence of the major dense line in myelin of the mutant mouse *shiverer*. *Neurosci. Lett.* 12:107–112.
35. Raine, C. S. 1984. Morphology of myelin and myelination. *In* Myelin. P. Morell, editor. Plenum Publishing Corp., New York. 1–50.
36. Readhead, C., B. Popko, N. Takahashi, H. D. Shine, R. A. Saavedra, R. L. Sidman, and L. Hood. 1987. Expression of a myelin basic protein gene in transgenic *shiverer* mice: correction of the dysmyelinating phenotype. *Cell.* 48:703–712.
37. Richardson, W. D., B. L. Roberts, and A. E. Smith. 1986. Nuclear location signals in polyoma virus large-T. *Cell.* 44:77–85.
38. Roach, A., K. Boylan, S. Horvath, S. B. Prusiner, and L. E. Hood. 1983. Characterization of cloned cDNA representing rat myelin basic protein: absence of expression in brain of *shiverer* mutant mice. *Cell.* 34:799–806.
39. Roussel, G., and J. L. Nussbaum. 1981. Comparative localization of Wolfgram W1 and myelin basic proteins in rat brain during ontogenesis. *Histochem. J.* 13:1029–1047.
40. Rumsby, M. G., and A. J. Crang. 1977. The myelin sheath – A structural examination. *Cell Surf. Rev.* 4:247–362.
41. Smith, P. R. 1978. An integrated set of computer programs for processing electron micrographs of biological structures. *Ultramicroscopy.* 3:153–160.
42. Smith, R. 1977. Non-covalent cross-linking of lipid bilayers by myelin basic protein: a possible role in myelin formation. *Biochim. Biophys. Acta.* 470:170–184.
43. Sternberger, N. H., Y. Itoyama, M. W. Kies, and H. deF. Webster. 1978. Myelin basic protein demonstrated immunocytochemically in oligodendroglia prior to myelin sheath formation. *Proc. Natl. Acad. Sci. USA.* 75:2521–2524.
44. Takahashi, N., A. Roach, D. B. Teplow, S. B. Prusiner, and L. Hood. 1985. Cloning and characterization of the myelin basic protein gene from mouse: one gene can encode both 14 kd and 18.5 kd MBPs by alternate use of exons. *Cell.* 42:139–148.
45. Trapp, B. D., T. Moench, M. Pulley, E. Barbosa, G. Tennekoon, and J. Griffin. 1987. Spatial segregation of mRNA encoding myelin-specific proteins. *Proc. Natl. Acad. Sci. USA.* 84:7773–7777.
46. Verity, A. N., and A. T. Campagnoni. 1988. Regional expression of myelin protein genes in the developing mouse brain: in situ hybridization studies. *J. Neurosci. Res.* 21:238–248.
47. White, J. G., W. B. Amos, and M. Fordham. 1987. An evaluation of confocal versus conventional imaging of biological structures by fluorescence light microscopy. *J. Cell Biol.* 105:41–48.
48. Wigler, M., A. Pellicer, S. Silverstein, R. Axel, G. Urlaub, and L. Chasin. 1979. DNA-mediated transfer of the adenine phosphoribosyltransferase locus into mammalian cells. *Proc. Natl. Acad. Sci. USA.* 76:1373–1376.
49. Yu, T.-T., and A. T. Campagnoni. 1982. *In vitro* synthesis of the four mouse myelin basic proteins: evidence for the lack of a metabolic relationship. *J. Neurochem.* 39:1559–1568.